SG Undersea Cable System:

Cable and Coupling Design

By G. E. MORSE, S. AYERS, R. F. GLEASON, and J. R. STAUFFER

This paper describes 1.7-in. SG submarine cable and cable termina-tions and compares their mechanical and electrical performance with the design objectives. At 30 MHz, transmission loss in the cable is very sensitive to variation in dielectric loss. Precautions required to prevent excessive dielectric loss change during cable manufacture and subse-quent system life are discussed. Sea-bed temperature and pressure coefficients are reviewed in the light of TAT-6 experience, and an es-timate is made of possible attenuation change over a 20-year inter-val.

I. INTRODUCTION

As discussed in the preceding papers, the British Post Office (BPO) had primary responsibility for cable development for the SG system and Bell Telephone Laboratories (BTL) was responsible for the repeater-to-cable coupling design.

A number of factors ruled out the use of 1.5-in. diameter-over-di-electric (DOD) SF[1] cable for the SG system; not least of these was its high loss. The channel capacity chosen for SG required an upper frequency of approximately 30 MHz. At this frequency, the attenuation of SF cable for a transatlantic system would have reached a formidable 32,600 dB but, by using a low-loss dielectric at an increased diameter, 1.7 in. DOD SG cable reduced this total by 5000 dB. This saved 123 repeaters and reduced the system power feed voltage.

However, cable attenuation remained far higher than on any previous system. This was reflected by: an increased sensitivity to manufacturing tolerances, significant attenuation changes with time (cable aging), and increased importance of laying effects and sea-bed temperature and

pressure coefficients. Of particular concern was the control and characterization of dielectric loss behavior. Surprisingly, the adoption of a low-loss dielectric seems to have compounded the difficulties and eventually came to dominate the cable development. This may be understood in part when it is appreciated that a change in dielectric loss-angle of 1 microradian on all the cable would cause a change of 26 dB at top frequency on TAT-6.

II. DESIGN OBJECTIVES

Many factors influence the design of a new cable. These include system costs, the development schedule, manufacturing capability, considerations of shipboard handling and maintenance, and compatibility with the repeater, its housing, and termination.

Early considerations of the possible lines of development indicated that, in the available time, a series of objectives based largely on modifications to the SF design would be the best approach. Economic studies showed that, for an upper frequency of 30 MHz, a more expensive cable with lower attenuation would reduce the total system cost in addition to increasing system reliability by reducing the number of repeaters.

The following improvements to the SF design were therefore set as general objectives.

(*i*) Reduce the cable attenuation at 30 MHz by the use of a larger cable and a lower-loss dielectric.

(*ii*) Reduce the dc resistance of the inner conductor by some 50 percent to offset the increased line current required by the SG repeater.

(*iii*) Increase the strength of the deep water cable to exceed, by at least 20,000 lb$_f$ (88.96 kN) the weight in water of 3000 fathoms (5486 m) of cable plus three repeater bodies.

(*iv*) Improve the handling performance in terms of the minimum safe bending radius and the number of reverse bends before the inception of a crack in the outer conductor.

Work in conjunction with Imperial Chemical Industries Ltd. (ICI) and Standard Telephones and Cables Ltd. (STC) showed that a dielectric material with a loss angle of 47 μrad at 30 MHz could be extruded satisfactorily at a diameter of 1.7 in. (43.18 mm), the cable dimension giving minimum system cost. The inner conductor retained the SF geometry with the diameter increased to 0.478 in. (12.14 mm) to meet the other essential requirements. This dimension gave the cable the convenient impedance of 50 ohms, which is very near to the value for minimum attenuation and provides a value of attenuation negligibly greater than the minimum.

With these basic parameters fixed, the more detailed objectives were formulated, and development concentrated on providing a detailed

specification for all stages of material supply, cable manufacture, and testing.

III. DESCRIPTION OF CABLE

A number of different cable designs are required to meet the wide range of laying stresses and operational risks that a long-distance, deep-water system must survive. To satisfy these requirements, five versions of 1.7 in. (43.18 mm) cable were developed: an armorless cable for deep water use, a light armored transition cable, a heavy single-armored cable, a heavy double-armored cable, and a screened cable.

3.1 Armorless deep sea cable

The main system cable (Fig. 1) is an armorless design protected by a polyethylene sheath and provided with an internal strength member. It is suitable for use in deep water where there is little risk of damage by fishing trawls, clam dredgers, and ships' anchors, or of disturbance and abrasion by ocean currents on a rocky sea bed. Cable to this design constituted 93 percent of TAT-6.

3.1.1 Inner conductor assembly

The strength member of the composite inner conductor consists of a 41-wire, high-tensile steel strand in which three layers of wires are arranged, all with a left-hand lay, around a central king wire. The design, shown in Fig. 2, is essentially a scaled-up version of the SD/SF strand with the wire sizes increased to give a nominal diameter of 0.4305 in. (10.93 mm). The previous distribution of bending stresses was retained at the increased diameter by increasing the lay length to 9.10 ± 0.35 in. (231.1 ± 8.9 mm). If steel wire with a tensile strength of 300,000 lb_f/-

HIGH-DENSITY POLYETHYLENE SHEATH WITH 2% CARBON BLACK, 0.175 IN. THICK, 2.070 IN. OD

MEDIUM-DENSITY LOW-LOSS POLYETHYLENE DIELECTRIC, 1.700 IN. OD

41-WIRE HT STEEL STRAND, 0.430 IN. OD

0.029 IN. THICK COPPER INNER CONDUCTOR 0.478 IN. OD
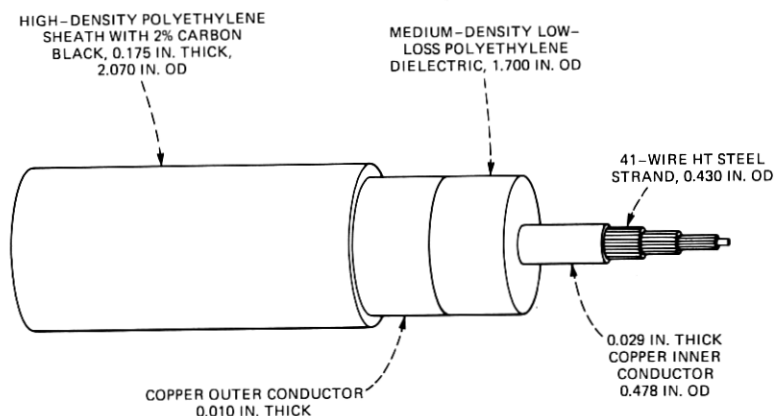
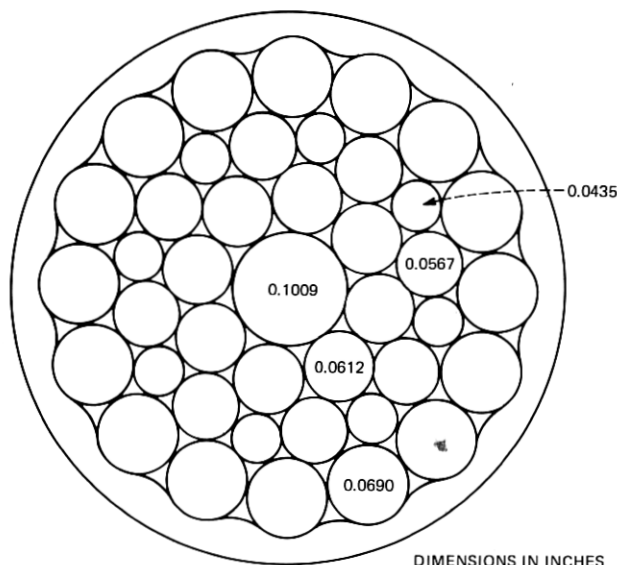COPPER OUTER CONDUCTOR 0.010 IN. THICK

Fig. 1—Armorless SG ocean cable.

Fig. 2—Cross section of inner conductor. The tolerance on the wires is ±0.0005 in., except for the center wire, where it is ±0.0010 in. The wire is high tensile steel, 291,200 to 336,000 lb_f/in² (2008 to 2317 MPa).

in² (2068.5 MPa) is used, the strand has a strength of 37,000 lb_f (164.6 kN). Based on an estimated weight in water of 3500 lb_f (15.57 kN) per nautical mile, this gives the cable a strength-to-weight modulus* of 10.6 nmi (19.67 km). The immersed weight of a repeater body is 550 lb (2446 N) so when three bodies are supported at a depth of 3000 fathoms the excess strength of the cable is nearly 25,000 lb_f (111 kN). This exceeds the design target by 25 percent without including the strength contribution of the other materials outside the steel strand.

The inner conductor is formed from a 0.029-in. (0.737 mm) thick, fully annealed, high-conductivity copper tape. It is wrapped around the strand, in tandem with the strand-forming operation, to produce an oversize tube. The tape edges are closed in a longitudinal butt joint which is seam-welded with an inert gas arc. The conductor is completed by drawing the tube tightly onto the strand to give a finished diameter of 0.478 ± 0.001 in. (12.14 ± 0.025 mm). The previous practice of specifying oxygen-free high conductivity copper was relaxed to allow the use of a cheaper high conductivity electrolytic tough pitch copper. To maintain weld quality and reliability, a minimum purity of 99.9 percent and maximum oxygen content of 0.05 percent were specified. A further

---

* The modulus of a cable is equal to the strength divided by the weight per nautical mile in sea water.

control was placed on the maximum size (0.0014 in., 0.036 mm) and dispersion of oxide grains. The minimum conductivity allowed was 100.8 percent as defined by the International Annealed Copper Standard (IACS).

To ensure that the copper-to-steel interlayer shear strength is sufficient to transfer laying and recovery stresses to the strength member, the copper is heavily swaged into the interstices of the strand. The thickness of copper immediately over the wires is reduced to 0.024 in. (0.61 mm), but the effective thickness of the conductor is held at 0.029 in. (0.737 mm) by suitable adjustment of the difference between tape feed rate and line speed. As a result of cold forming, the conductor tape is work-hardened, and its conductivity is reduced on an average by 1.2 percent. This is later offset by approximately 0.35-percent increase due to a partial anneal during core extrusion. In the design model, a final conductivity of 99.5 percent IACS was assumed. This value was set low to ensure that sufficient repeaters were ordered. In TAT-6, the mass conductivity, determined from 119 samples of finished inner conductor, was 100.2 percent IACS. This result assumes a value of 8.89 g/cm^3 for the density of copper. If account is taken of the true density, then the volume conductivity would appear to have been slightly higher at about 100.4 percent IACS. The design value for the inner conductor resistance was 0.911 ohms per nautical mile at 10°C. Cable manufactured for TAT-6 in fact came out slightly higher at 0.931 ohms per nautical mile because the conductivity of the steel was lower than expected.

3.1.2 Dielectric

As system bandwidths are increased, the dielectric loss becomes more significant. Its contribution to cable attenuation is proportional to the product of loss angle and frequency and is independent of cable size, whereas the contribution from the conductor loss is inversely proportional to cable diameter and, once skin effect is established, is substantially proportional to the square root of frequency. The effect of dielectric loss at high frequencies is to increase cable attenuation and accentuate the deviation from a root frequency law, particularly in large diameter cables, thus complicating the compensation of manufacturing deviations by length adjustment.

In cable used for SF at 6 MHz, the dielectric was responsible for only 3 percent of the total loss at the top of the band, but using this polyethylene in SG cable increases the proportion to 10 percent at 30 MHz. To gain a worthwhile improvement, it was necessary to halve the dielectric loss while maintaining the other essential properties. Two UK suppliers, ICI and Bakelite Xylonite Ltd (BXL), met this requirement during the development stage and UBE Industries of Japan was approved during TAT-6 cable production.

Table I — Loss angle requirements

Frequency (MHz)	Loss Angle in Microradians at 23°C	Change from 23° to 3°C
30	47 ± 6	11 ± 2
	Loss angle expressed as a proportion of the loss angle at 30 MHz, 23°C	
1	0.62 ± 0.14	
6	0.77 + 0.10 −0.14	

The selected dielectric is a high molecular weight polyethylene characterized by a low contamination level, a precisely controlled permittivity, and a low dielectric loss. The reduction in loss was achieved by raising the density to 0.930 g/cm^3 (thus reducing the amount of amorphous material contributing to the loss), reducing the concentration of polar groups, and controlling more closely other impurities and adventitious contamination. Although approximately 3 μrad of the reduced loss angle was offset at 30 MHz by an increase in permittivity caused by the increase in density, the shift from SF to SG polyethylene is responsible for a net reduction in TAT-6 cable loss of 1300 dB at 30 MHz. The nominal* SG polyethylene loss angle is shown in Table I.

The tolerance at 1 and 6 MHz was expressed as a proportion of the 30-MHz value to control the shape of deviations in the linear frequency loss term while, at the same time, allowing the material suppliers a reasonable margin. A control on the loss-angle change with temperature was specified to limit the uncertainty in sea-bed loss at 30 MHz and to avoid a multiplicity of cable coefficients.

To allow for some small variation among sources of material, the quality assurance control was related to the nominal values of each material as determined during the type approval process. However, in approving alternative polyethylenes, the need to process them under similar conditions was appreciated; hence, close controls were placed on those properties affecting extrusion characteristics. Thermal oxidation was controlled by the low-loss antioxidant used in SF cable—Ethyl Antioxidant 330 [1, 3, 5 trimethyl-2, 4, 6 tri (3, 5-ditertbutyl 4-hydroxy-benzyl) benzene]. As a further protection against thermal oxidation, the granule feed hopper to the extruder screw was flooded with nitrogen. The increased density and crystallinity of the low-loss material led to a reduction in its stress crack resistance, but the level achieved was considered acceptable in view of the protection provided by the sheath and outer conductor and the absence of any record of a service failure due to stress cracking.

---

* The nominal loss angle of SG polyethylene at 30 MHz is based here on the value obtained with the Bell Laboratories Murray Hill test set. The Bell Laboratories set was used as the reference against which the dielectric test sets at the polyethylene suppliers and the two cable factories were calibrated by a careful exchange of plaques.

The polyethylene is pressure-extruded over the inner conductor and cooled in a series of water troughs which successively reduce the core temperature to the factory ambient (further details are given in Section V). The rate of cooling is arranged to prevent retraction of the core from the inner conductor. By this means, the interlayer adhesion required to transfer longitudinal laying stresses to the inner strength member is maintained. During development, the interlayer shear strength over a 3-in. length of conductor typically varied between 500 and 1000 lb$_f$ (2225 and 4450 N) and occasionally reached 2000 lb$_f$ (8900 N). However, under production conditions, the adhesion achieved over the same length varied between 250 and 500 lb$_f$ (1112 and 2225 N). The required adhesion was 225 lb$_f$ (1000 N). After extrusion, the dielectric is shaved to a diameter of 1.700 ± 0.003 in. (43.18 ± 0.076 mm) at a temperature of 20°C. The eccentricity of the inner conductor is limited to 0.020 in. (0.51 mm).

3.1.3 Outer conductor and sheath

The outer conductor is fabricated from an annealed copper tape, 0.010 ± 0.0005 in. (0.254 ± 0.0127 mm) thick by 5.630 ± 0.010 inch (143.0 ± 0.254 mm) wide, having essentially the same properties as the inner conductor tape. It is wrapped tightly around the shaved core at a temperature of 20 ± 1°C with the edges overlapped longitudinally by approximately 0.25 in. (6.35 mm). The maximum stretch permitted in the forming process is 0.5 percent. To provide the conductor with support and protection, it is oversheathed in a tandem operation with high-density polyethylene to a diameter of 2.07 ± 0.03 in. (52.58 ± 0.76 mm). To ensure adequate bending performance and avoid alignment problems when jointing, the minimum sheath thickness was limited to 0.150 in. (3.81 mm) and maximum eccentricity to 0.020 in. (0.51 mm).

In the design model, a conductivity of 100.5 percent IACS was assumed for the outer conductor, but during TAT-6 production an average mass conductivity of 100.8 percent IACS was measured on 121 samples. This figure becomes 101.0 percent IACS if a correction is made for the error in assumed density. The average dc resistance for the entire production run was 0.836 ohms per nautical mile at 10°C.

During development, the bending performance of three outer conductor thicknesses, 0.008, 0.010, and 0.012 in. (0.203, 0.254, and 0.305 mm), was examined in combination with three sheath thicknesses, 0.125, 0.150, and 0.165 inch (3.175, 3.81, and 4.19 mm). A wide variation was found among cable samples having the same outer conductor and sheath thickness, which made comparison difficult. In general, the resistance to buckling and cracking improved as the conductor and sheath thicknesses increased, but the thicker the conductor the more pronounced the effect of the sheath. Each combination was assessed from flex tests but the extent of bending damage was very dependent on the test rig

used. There was also a marked improvement in bending performance when the bending diameter was increased from 9 to 10 ft (2.74 to 3.05 m). These differences were considered sufficient to justify setting 10 ft (3.05 m) as the bending limit for 1.7-in. (43.18 mm) cable.

The performance of the 0.008-in. outer conductor was very marginal at a bending diameter of 10 ft (3.05 m) and it failed to survive 50 reverse bends in every test at 9 ft (2.74 m) irrespective of sheath thickness. The selected combination of 0.010/0.165 in. (0.254/4.19 mm) was also slightly marginal, but the risk was thought to be acceptable provided the minimum sheath thickness did not fall below 0.150 in. (3.81 mm).

The sheath material was a high molecular weight, high-density ethylene copolymer, containing 2.6 percent by weight of carbon black. The density specified was slightly higher than that required in SF cable. This increased the flexural modulus which increased the hoop stress applied to the outer conductor by the sheath, thus improving the reverse bend performance. Four sources of sheath material were approved, although only three were used in TAT-6. Towards the end of production, the inclusion of carbon black as protection against actinic radiation was discontinued except for cables ordered as repair lengths. Ironically, the removal of carbon black brought a substantial improvement in bending performance. In continuous loop tests, where cable is driven in a figure eight between two sheaves, the onset of cracking at 6-ft (1.83 m) diameter changed from 20 to 40 reverse bends and at 10 feet (3.05 m), cracking did not occur before 100 reverse bends. Clearly, the use of a natural sheath material opens up the prospect of a useful cost saving in future systems from the use of a thinner conductor/sheath combination. However, those responsible would be well advised to retain the original dimensions for repair lengths containing carbon black. In the final design, the weight in sea water was 1.6 tons* per nautical mile and in air 5.7 tons per nautical mile. The strength was 16.5 ton$_f$ and the modulus 10.5 nmi (19.5 km).

3.1.4 Jointing

Shipboard and factory joints were developed along separate lines to take account of differences in the conditions and equipment available for their preparation. For example, while both share a common standard for tensile strength and bending performance, completion of a shipboard joint is required in the shortest possible time.

Both methods use a swaged steel ferrule to make a joint in the inner conductor assembly, and each type of joint has a minimum strength of 15 ton$_f$. In the factory, this is achieved using a 6.5-in. (165.1 mm) long ferrule pressed to a mean diameter of 0.82 in. (20.8 mm) and in a repair by swaging a 4.5-in. (114.3 mm) long ferrule to a diameter of 0.87 in. (22.1 mm). With these dimensions, there is little to choose between them

---

* 1 ton = 2240 lbs, or 1016 kg.

electrically. The factory ferrule has a return loss at 30 MHz of 20 dB compared with 21.5 dB for the shipboard version.

The dielectric is restored using an injection molding process, and both versions must be capable of withstanding 200 kV dc for 1 minute in type approval tests. All core joints are examined radiographically for voids, cracks, and inclusions. Each joint made in the factory must also withstand a production test of 100 kV dc for 1 minute without failure. In a shipboard joint, the outer conductor is connected through by the insertion of a split copper wire braid soft-soldered to the parent outer conductor. While this technique has a superior bending performance to the SF outer conductor restoration, lingering doubts regarding its long-term electrical stability have prevented its adoption for factory use. To improve the flexibility of the outer conductor restoration, instead of spot-brazing a split copper tube directly to the outer conductor as in SF, three helical copper tapes are spot-brazed to the split tube and to the outer conductor. This provides a semiflexible connection which, in a complete joint, is capable of withstanding 50 reverse bends at a diameter of 10 ft (3.05 m) without loss of continuity. In the factory, the joint is completed by fusing a split section of sheath to the cable and sealing it with a longitudinal seam weld. The hoop stress of the sheath is restored by a tight, close-wound binding of $\frac{1}{16}$ in. (1.59 mm) galvanized iron wire for a distance of 5 ft (1.52 m) over the joint. For the shipboard joint, the sheath is restored by a polyethylene sleeve slipped on the cable and located over split sheath sections placed as packing over the braid. The ends of the sleeve are fused to the sheath in an injection mold and reinforced with a galvanized wire binding.

3.1.5 Pre-formed dead ends for holding armorless cable (stoppers)

When holding armorless cable during a repair, it is necessary to grip the cable by a method that transfers the load from the inner strength member to the dead end without causing damage to the cable. This is arranged using a dead end manufactured by Preformed Line Products (GB), Ltd, Andover, England. In essence, thirteen 0.212-in. diameter high tensile steel wires are formed into a helical tape 26 ft long. The wires are fixed together with a vinyl adhesive and coated on the inside of the helix with aluminum oxide. By reversing the lay of the helix at the middle of the tape, the ends may be folded into a hairpin which, when wrapped around a cable, leaves a convenient loop for the attachment of a shackle.

A single dead end is capable of holding armorless cable at tensions up to 18 ton$_f$ but, if cable is held at the bow of a ship for long periods, tension, bending, and vibration fatigue may cause premature outer conductor failure well below this value. Since a splice may take several hours to complete, the use of two dead ends in tandem, linked by an equalizing sling to spread the load, is essential.

With careful protection of the cable at the eye of each dead end, it is possible to hold SG cable for 12 hours under a cyclic load of 1 to 7 tonf with a period of 6 seconds. However, if the tension range is increased to 1 to 9 tonf, the time to develop fatigue cracks in the outer conductor is halved.

3.2 Armored cable

In shallow water, additional protection is required to prevent cable failure due to abrasion or disturbance by fishing trawls and ships' anchors. This may be achieved by the provision of a suitable armor or by cable burial depending on the circumstances. Since the TAT-6 route was suited to cable burial using a plow, it was planned to maximize protection by laying heavy single-armored cable to a depth of 1000 fathoms (1829 m) and by burying the cable at depths less than 500 fathoms (914 m). Clearly, the description "shallow water" is something of a misnomer, but the need for protection is real. Fish are now caught at 800 fathoms (1460 m), and a trawl fault has occurred at a depth of 735 fathoms (1340 m). In TAT-6, the plow was used to a maximum sea-bed depth of 350 fathoms (640 m), while the transition to armorless cable was made at 750 fathoms (1372 m). However, a short length of single-armored cable was successfully laid at 1100 fathoms (2012 m) when the depth briefly increased after the transfer from armorless to armored cable on completion of the deep sea lay.

When low attenuation is not a prime requirement, operational constraints during laying and repair favor the choice of a small diameter coaxial for the armored cable. However, during the SG development the feasibility of armoring the main system cable was demonstrated and on a sea trial this cable was laid and recovered without serious difficulty. Indeed, the feasibility of using a heavy double-armored 1.7-in. cable was also demonstrated. The 1.7-in. cable was selected because its greater strength and weight provided increased protection from trawler attack and also because its use reduced the number of repeaters required.

3.2.1 Single-armored cable

To reduce the risk of an insulated break in the inner conductor and the attendant difficulty in location, it is customary in the design of armored cables to provide a ductile conductor that more than matches the elongation characteristic of the armor. In SG, the continued use of solid copper was prohibitively expensive, but there was insufficient time to develop an alternative* structure with high elongation before TAT-6 was laid. As a result, the TAT-6 armored cable used the high tensile steel strand inner conductor assembly of the armorless cable. It was therefore

---

* See possible alternatives in Section 3.2.3.

necessary to select the armor material with some care. The use of Grade-65 (British Standard abbreviation) medium tensile steel wire armor gives a residual strength* well below the minimum strength of the strand at a strain equal to the yield strain of the strand. In practice, the strand yields at approximately 1 percent strain when the armor has a residual strength of 11 ton$_f$. Since the minimum strength of the strand is 16.5 ton$_f$, its failure under load will cause a cable break and exposure of the inner conductor to the sea. The armor has a minimum strength of 68 ton$_f$; therefore, taking into account the contribution from the strand, the effective strength of the cable is 73.5 ton$_f$. In proving trials, the inner conductor integrity was demonstrated at tensions up to 79 ton$_f$ with failure occurring at approximately 0.8 percent strain.

The single-armor design is shown in Fig. 3. It comprises 25 wires of 0.291 ± 0.004 in. (7.391 ± 0.102 mm) diameter, medium tensile galvanized steel applied with a left-hand lay of 36.5 ± 1.0 in. (927 ± 25 mm) over a bedding of 75-pound (34 kg) jute. The armor is coated with bitumen and bound with two servings of 3-ply, 28-pound (12.7 kg) jute applied in opposite directions and coated with a bituminous compound to a finished diameter of 3.05 in. (77.5 mm). The cable specification in fact allowed the use of an approved alternative to jute and, since the completion of TAT-6, synthetic yarns have replaced it as the preferred bedding and serving material.

The single-armored SG cable has a weight in sea water of 15 tons per nautical mile and a weight in air of 24 tons per nautical mile. It is clearly not a cable that a small repair ship could handle easily but, provided the serving remains intact, it is relatively docile and can be coiled in a tank to a diameter of 12 ft (3.66 m) and drummed without difficulty at a diameter of 10 ft (3.05 m).
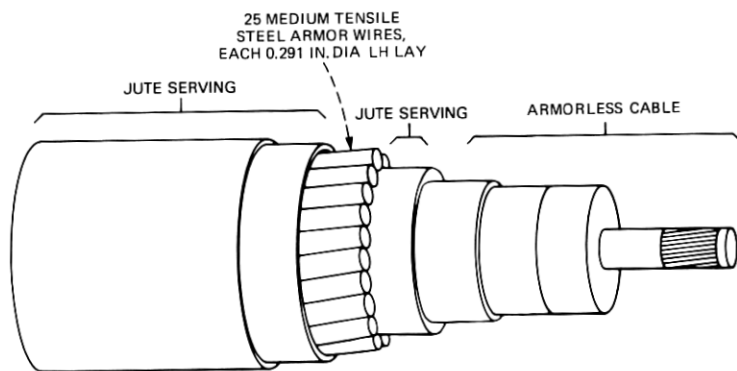

Fig. 3—Single-armored SG cable.

---

* Residual strength is the difference between breaking strength and the strength at a particular value of strain.

3.2.2 Transition cable

Since the static weight in water of single-armored cable at 1000 fathoms (1828 m) approaches very nearly the strength of the armorless cable, a light-armored transition cable is required at a transfer from armored to armorless cable. In the absence of previous experience of laying heavy-armored cable at this depth, it was considered advisable to provide a double-armored transition cable with a neutral torque characteristic. The design strikes an optimum strength-to-weight modulus of 2.6 nmi (4.82 km) for the armorless cable with respect to the transition cable and for the transition cable with respect to the single-armored cable. (That is, the armorless cable has strength to support the weight in water of 2.6 nmi of transition cable and, similarly, the transition cable has strength to support the weight in water of 2.6 nmi of single-armored cable.)

The transition cable is shown in Fig. 4. Each layer of armor has 48 Grade-65 galvanized steel wires coated with polyvinyl chloride to space the wires uniformly around the cable. In the first layer, the wires are 0.085 ± 0.001 in. (2.159 ± 0.025 mm) diameter applied with a left-hand lay of 42 ± 1 in. (1067 ± 25 mm) and in the second layer they are 0.078 ± 0.001 in. (1.981 ± 0.025 mm) diameter applied with a right-hand lay of 54 ± 1 in. (1372 ± 25 mm) over an intermediate serving comprising two opposing layers of 3 × 17 pound (7.7 kg) jute coated with bitumen. The cable is completed with an outer serving of two opposing layers of 3 × 28 pound (12.7 kg) jute flooded with a bituminous compound to an overall diameter of 3.17 in. (80.5 mm). Its weight in sea water is 5.9 tons per nautical mile, and its weight in air is 15.5 tons per nautical mile.

The armor strength varies from 21 to 25.8 ton$_f$, depending on the quality of steel, but because the inner conductor fails at 1-percent strain, only about 88 percent of the potential strength is realized. The combined strength of the armor and strand therefore varies from 35 to 39.2 ton$_f$.
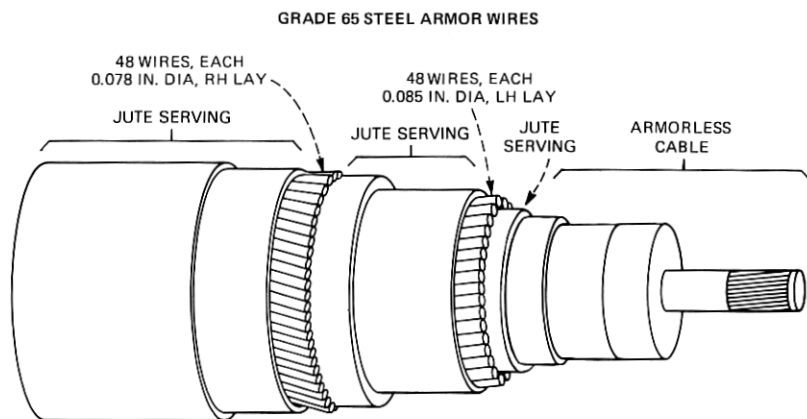
GRADE 65 STEEL ARMOR WIRES

Fig. 4—Transition cable.

In proving trials, failure occurred at 39 ton$_f$ with an extension of 0.84 percent. No rotation of the armor was observed.

3.2.3 Double-armored cable

As stated previously, the feasibility of laying a double-armored SG cable was demonstrated but such a cable was not adopted for TAT-6. The bedding and first armor pass is as for the single-armored cable. Then, with coatings of bituminous compound under and over each layer, two intermediate servings of 3-ply 17-lb (7.7 kg) jute are specified with opposing lays. This is followed by a second armor pass of 33 wires, 0.291 ± 0.004 in. (7.391 ± 0.102 mm) diameter, Grade-65 medium tensile galvanized steel, applied with a left-hand lay of 48 ± 1 in. (1219 ± 25 mm). The second pass is served with two opposing layers of 3-ply 28-lb (12.7 kg) jute coated in bitumous compound to ensure that the serving adheres firmly to the armor. The finished cable has a weight of 32.8 and 46.8 tons per nautical mile in sea water and air respectively and an overall diameter of 3.8 in. (96.5 mm). It has a tensile strength of 162 ton$_f$.

The tremendous strength of this cable rules out the use of a composite inner conductor with a high tensile steel strand if an insulated inner conductor break is to be avoided. However, preliminary trials of a 19-wire mild steel strand and of copper-clad aluminum rod indicate that either could be used, the former with virtually no further development.

3.3 Screened cable

At shore ends and in land sections, additional screening is required against electromagnetic interference in the low-frequency band. In SG, the primary concern is with the radio broadcast band, 0.55 to 1.6 MHz. At these frequencies, adequate protection is given by increasing the outer conductor thickness to 0.030 in. (0.762 mm). This was shown to be practicable towards the end of SG development and may be used in future systems, but in TAT-6 a modified version of the SF screened cable[1] was used. The cable impedance was converted to 50 ohms by increasing the inner conductor diameter to 0.281 in. (7.137 mm). Corrosion-prone neoprene-covered armor wire was replaced by a conventional armor, protected with tar and jute servings.

IV. ELECTRICAL CHARACTERIZATION

To enable the system to be equalized, the level of uncertainty in the predicted attenuation of laid cable must be reduced to that which can be corrected by the ocean-block equalizer (OBE). While many factors contribute to uncertainty, some tend to be random while others are systematic. The random factors include manufacturing variations and measurement error. An error in the temperature or pressure coefficient, on the other hand, will cause a systematic deviation from the predicted

sea-bed loss. In the OBE, provision was made for the correction of cable misalignment amounting to ±2.5 dB systematic and ±1.5 dB random per ocean block at 30 MHz. In a 20-repeater block, this corresponds to a total of ±0.48 percent of cable loss.

Since cable and repeater development proceeded simultaneously, predictions of cable loss and laying coefficients were required in advance of the manufacture of experimental cable sections. The initial estimates were provided from theoretical consideration of the physical properties and dimensional behavior of cable material based on experience with SD and SF systems and supplemented as necessary by experimental data of dielectric loss at frequencies up to 30 MHz. Uncertainties in sea-bed estimates were narrowed in the light of experience gained from sea trials and refined again as experimental data led to a better understanding of the results. The objective was the characterization of cable typical of large-scale production rather than the accurate description of experimental lengths.

4.1 The effect of variation in manufacture

Strict control of material properties, cable dimensions, and manufacturing processes is exercised through the cable specification, in order to limit the variation in cable loss. Table II shows the potential magnitude of variations due to raw material and dimensional tolerances. In the case of conductivity, no advantage is to be gained from an upper limit, so the anticipated variation is shown. A similar situation exists with the

Table II — Effect of variation in material properties and cable dimensions on cable attenuation

		Effect on Attenuation in Percent		
Parameter	Tolerance	1 MHz	6 MHz	30 MHz
Inner conductor:				
Diameter	±0.001 in. (±0.025 mm)	±0.00	±0.00	±0.00
Thickness	±0.0005 in. (±0.013 mm)	±0.00	±0.00	±0.00
Conductivity	±0.4%	∓0.15	∓0.15	∓0.15
Core insulation:				
Diameter	±0.003 in. (±0.076 mm)	∓0.18	∓0.18	∓0.17
Relative permittivity	±0.004	±0.09	±0.09	±0.09
Loss angle: 30 MHz	±6 μR	—	—	±0.57
6 MHz	+ 5.5 μR / −7.4 μR	—	+0.24 / −0.33	—
1 MHz	±7.4 μR	±0.14	—	—
Outer conductor:				
Air gap	±0.0006 in. (±0.015 mm)	∓0.11	∓0.10	∓0.10
Thickness	±0.0005 in. (±0.013 mm)	±0.00	±0.00	±0.00
Conductivity	±0.4%	∓0.04	∓0.04	∓0.04

air gap* between the core and outer conductor. Although it cannot be quantified by the specification, every attempt is made to control and regulate its size. It is perhaps worth commenting that the limits on diameter and permittivity variation were met in every cable section manufactured for TAT-6 (the former by a fair margin), and that the polyethylene core material met the loss angle requirement in more than 97 percent of the cable sections.

4.2 Control of deviation from design

With one exception, the effect of individual tolerances is small, but when combined they amount to a total deviation of ±1.2 percent at 30 MHz. Half of this is due to the dielectric loss, but since its effect at low frequencies is far less, equalization at 30 MHz by length adjustment will cause a significant deviation from design in the low band. This was thought to be sufficient justification for a further control on the final characteristic. When the first experimental cable lengths were produced, another reason emerged.

Attenuation measurements on trials cables revealed an enhanced loss which had every appearance of being due to the dielectric but which proved difficult to confirm from dielectric loss measurements on samples prepared from extruded core. The apparent[†] increase in loss angle was 7 to 8 μrad at 30 MHz. Since this had a significant impact on attenuation, it was incorporated into the design model. It became necessary therefore to provide a means of checking that the effect remained constant during production. This was achieved by extracting the apparent loss angle of the cable at 30 MHz from an examination of the ratio of the losses at 30 and 1 MHz using the following expression:

Apparent loss angle at 30 MHz = $57 + 188(R - 5.756)$ μrad,

where

$$R = \frac{\text{measured insertion loss (dB) at 30 MHz}}{\text{measured insertion loss (dB) at 1 MHz}}.$$

It can be shown from consideration of the transmission equations that the ratio R is proportional to the loss angle at 30 MHz but relatively independent of it at 1 MHz. It is also virtually unaffected by deviations in loss which are "cable shape." Combining errors from all sources, including test equipment, the technique is considered accurate to ±1.7 microradians at 30 MHz. By smoothing the measured data, it is possible

---

* The outer conductor does not conform precisely to the surface of the dielectric; the term "air gap" refers to the space between the outer surface of the dielectric and the inner surface of the outer conductor. The thickness of the air gap is the average value of the separation between these surfaces.

† The apparent increase in loss angle is now thought to be due in part to a calibration error of 5 μrad in the reference dielectric test set. It is hypothesized that the remainder is due to oxidation or contamination of the polyethylene during core extrusion.

to reduce this uncertainty to ±1 microradian. Given that the dielectric as supplied remains within tolerance, then the apparent loss angle should not vary by more than ±8 μrad from a nominal value of 62 μrad at 10°C. This proved to be the case, but it was soon found that a tolerance of this magnitude allowed large variations in the change of dielectric loss between raw material and finished cable resulting from differences in manufacturing conditions. Since this had an adverse effect on subsequent loss stability, the control was placed instead on the processing change. This was implemented by restricting the change between raw material measured at 23°C and finished cable measured at 10°C to 14 ± 4 microradians. To give an early warning of approaching trouble so that immediate remedial action could be taken, the use of moving range control charts showing the dielectric process change was made mandatory toward the end of TAT-6 production.

Having extracted a value for the dielectric loss at 30 MHz, the combined deviation of the cable shape components of cable loss can be estimated and controlled. A tolerance of ±0.5 percent was specified which encompassed the total production deviation from the mean characteristic at each factory.

It is evident from Table II that small variations in the air gap could be responsible for a sizeable "laying effect," i.e., the amount by which the cable misses its sea-bed design loss. To check that the application of the outer conductor was under control, one section in 10 was required to be repanned (removed from one storage pan and coiled into another) after the factory transmission tests and then remeasured. A large increase in loss as a result of handling the cable would point to a slack outer conductor and the need for adjustment of the forming mill.

In the final design loss for factory measurements at 10°C, shown in Fig. 5, an air gap of 0.0020 in. (0.051 mm) was assumed. In repanning operations, the air gap collapsed on the average by 0.0007 in. (0.018 mm) after a single turnover and by a further 0.0002 in. (0.005 mm) following a second turnover. However, the degree of scatter was fairly large and appeared to be related to previous storage conditions and the time elapsed before turnover.

4.3 Sea-bed coefficients

Laying coefficients to allow correction for temperature, pressure, and handling effects were obtained from 18 nmi (33.4 km) of prototype SG cable manufactured by STC. The trials cable was produced in four equal lengths, half with ICI and half with BXL low-loss polyethylene. The temperature coefficient was determined from transmission measurements of individual and paired lengths at five equally spaced temperatures varying from 22° to 4°C.

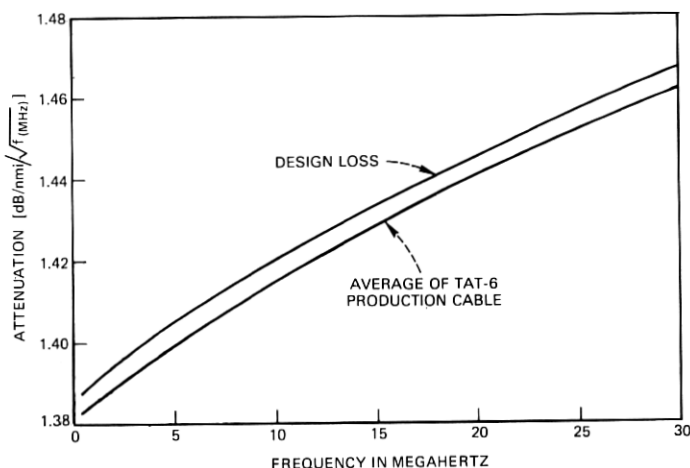At high frequencies, the cable temperature coefficient is increasingly

Fig. 5—Attenuation at 10°C and 0 fathom. An air gap of 0.002 in. between the outer conductor and core was assumed in the calculation.

dependent on the dielectric loss, but there was little evidence of difference among the SG dielectrics. The mean of the trials cable coefficients is compared in Fig. 6 with the final design coefficient. This is split into two parts to allow for laboratory evidence which suggested that the rate of thermal expansion of the dielectric differed over the temperature ranges 2.5° to 10°C and 10° to 20°C. However, a measured temperature coefficient was liable to apparently substantial but quite illusory modification by small variations in outer conductor behavior. If the direction of temperature change was from low to high, then the outer conductor did not move until the air gap closed. This caused an apparent increase in the temperature coefficient by overriding part of the dielectric contribution. An apparently nonlinear coefficient was readily caused by excessive delay between two measurements at successive temperatures. This allowed additional collapse of the outer conductor as the sheath very gradually contracted. A similar effect could be produced by successively overshooting and overcorrecting several times before reaching a stable temperature. The time constant of these effects was far longer than that required for dc resistance stabilization.

4.4 Sea trial

Having established the temperature coefficient, a sea trial was conducted in June 1973 by Cable Ship *Alert* to determine the pressure coefficient of the armorless cable and to assess the handling characteristics of the armored cable. The two 9-nmi (16.7 km) lengths of armorless cable were laid at depths of 1500 and 2500 fathoms (2743 and 4572 m) in the form of a hairpin, keeping both ends on board to facilitate trans-
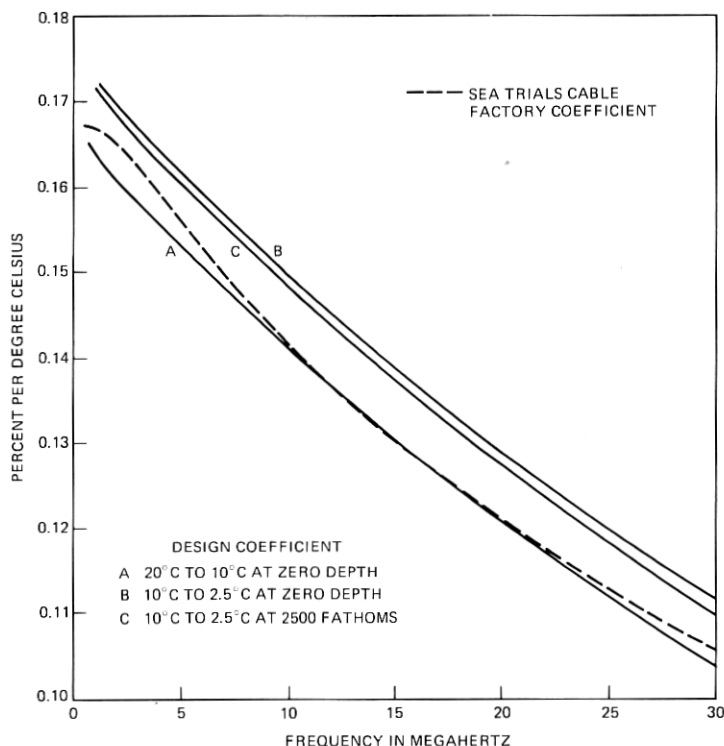
CABLE AND COUPLING **2451**

Fig. 6—Attenuation temperature coefficient for 1.7-in. SG cable.

mission tests. The design coefficient shown in Fig. 7 was based on the two points obtained from each cable measurement. The depth coefficient increased with frequency due to the increased influence of the dielectric. The coefficient obtained from the ICI cable was smaller than that from the BXL and, at 1 MHz, was 0.12 percent lower than the computed value for SF cable. It was therefore decided to bias the SG design coefficient towards the BXL characteristic with a value slightly above the SF design at 1 MHz.

The curve in Fig. 7 labeled "Mean Sea Trials Cable Coefficient" was calculated using additional depth information gained from downrunner* measurements. These were taken when the cable just reached the sea bed at each depth. The sea-trial cable coefficient is the average of a linear fit through the four points thus obtained for each length. Treated in this way, the ICI and the BXL data confirm the previous ICI two-point coefficient. The data also indicate the presence of a large air gap in the BXL cable which is consistent with the attenuation change seen during handling operations.

---

* The downrunner is the portion of cable between the ship and the sea bed.
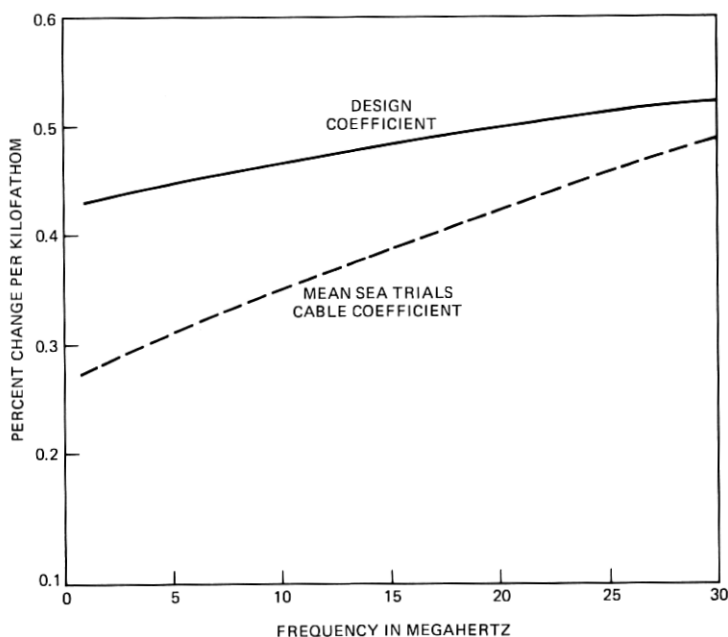
Fig. 7—Attenuation pressure coefficient for 1.7-in SG cable.

The essentially non-depth-dependent component of the pressure coefficient due to closing the air-gap under the outer conductor was modeled from air-gap behavior determined from laboratory measurement and sea trials results. The design value was set at 0.37 percent flat with frequency.

After the sea trials, both cables were streamed (laid out on the sea bottom), one at each depth, with a view to recovery at a later date to assess their stability over the intervening time period. This was undertaken in June 1975 by Cable Ship *John W. Mackay*. During the two-year interval, the cable which had been manufactured under conditions closest to those approved for TAT-6 production had increased in loss by the equivalent of 1 μrad at 30 MHz.

V. ANOMALOUS DIELECTRIC LOSS INVESTIGATION DURING TAT-6 CABLE PRODUCTION

When cable production started at CDL*, it was found that some freshly produced lengths exhibited excessively high apparent loss angles at 30 MHz, 20 to 30 μrad above nominal. It was quickly discovered that the effect was related to extruding core into an initial trough of water

---

* Cables de Lyon, Calais, France.

at 105°C† instead of the then accepted value of 95° to 97°C, as shown in Fig. 8. The higher temperature had been chosen to maintain adhesion and freedom from voids at increased extrusion line speeds. As a result of the investigation described below, the subsequent extruded core was chilled in a first water trough having a temperature of 92°C.

The high apparent loss angle of the affected cable continued to increase with time in the factory, appearing to reach a peak value after three to six months and then showing signs of slowly decreasing. When the temperature of the water in the first trough was reduced to 97°C, cable was produced within specification but some changes in apparent loss angle with time still remained (see Fig. 9). This resulted in lengthy investigations into the effects of water on polyethylene.

Freshly produced core, extruded into water at 97°C, was rushed from the factory to the laboratory and water measurements were made on three concentric layers. The outer layers were found to contain up to 200 parts per million (ppm) of water, while the other layers contained close
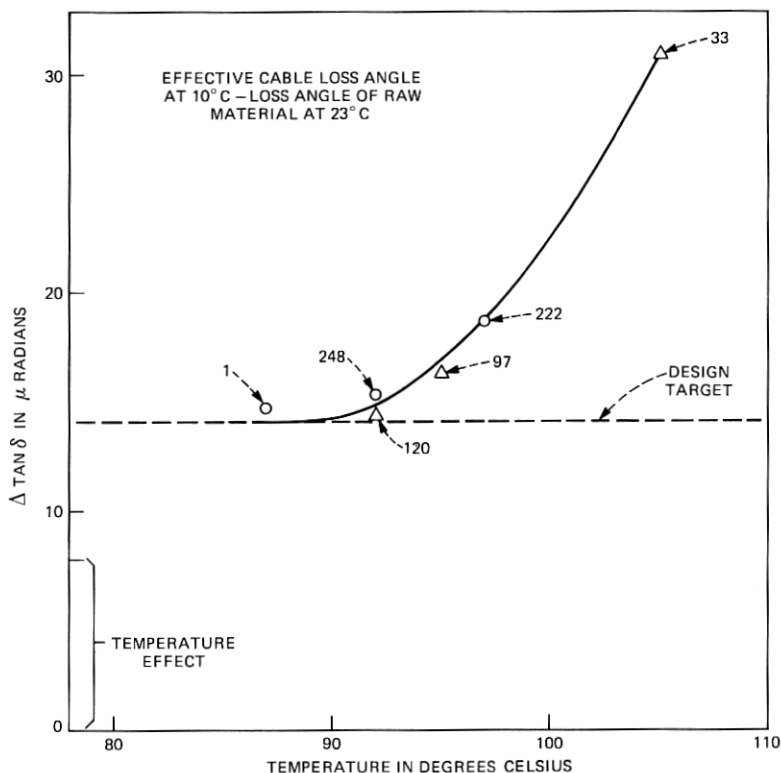

Fig. 8—Core extrusion cooling temperature versus loss angle change. Number of cable sections represented by each plot is shown on the curve.

† Pressurized cooling troughs allow temperatures above the atmospheric pressure boiling point.
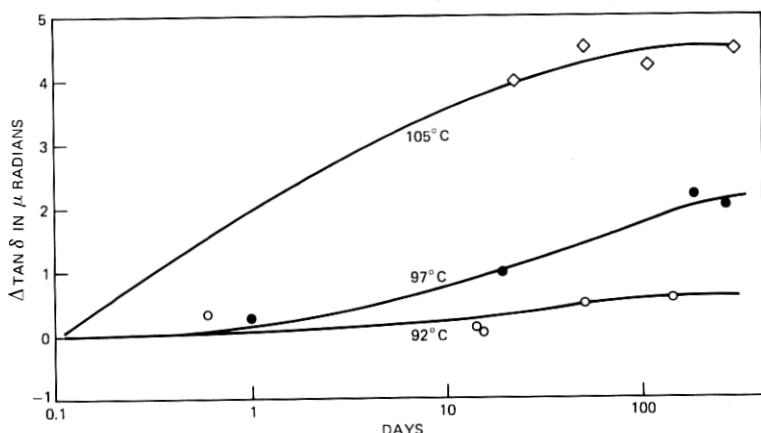
Fig. 9—Typical factory aging characteristic for cable core cooled at different temperatures. Change in apparent cable loss angle with time at 30 MHz and 10°C.

to the normal saturation levels of about 10 ppm at room temperature. Plaques were also molded from material from these three layers and the loss angles determined at several frequencies. Plaques from the outer layers of the core initially showed enhanced loss angles with an excess of 20 to 30 μrad at 30 MHz, but the values decreased quite rapidly with time, recovering to expected values within 24 hours.

5.1 Water measurements

As a result of this initial work, techniques were developed for examining the quantity and nature of the water trapped in the core. A cutter was produced which could remove a cylindrical plug from a cable core without affecting the distribution of water. If six of these plugs were used and sliced into thin disks, the radial distribution of the water in the core could be measured using a DuPont moisture analyzer to an accuracy of ±5 percent or ±2 ppm for small quantities of water. The distribution of water through a fresh core of SG polyethylene is given in Fig. 10. Most of the water is concentrated in the outer layers and is far in excess of normal saturation levels. It was suspected that the excess water was clustered in the form of microdroplets in small voids less than 1 μm in size. A Perkin-Elmer scanning calorimeter was used to confirm this theory of clustering. By cooling samples to −55°C and then monitoring them while gradually heating to 30°C, a peak in heat capacity was observed at 0°C caused by the melting of ice crystals formed where the water had clustered. The quantity of clustered water was calculated from the enthalpy of fusion of frozen water. Attempts to see the microdroplets under a microscope proved unsuccessful, although clusters 2 μm in diameter were detected when plaques were subjected to high-pressure steam and quenched in water at 23°C. This supports the suggestion that

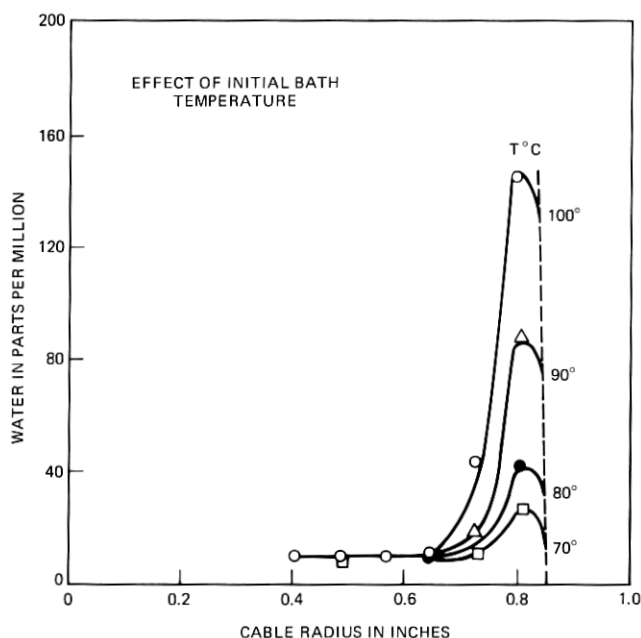Fig. 10—Distribution of water through an SG cable core.

the microdroplets produced under normal, less severe conditions are smaller than 1 μm.

The techniques described above were used to determine the quantity of both the total and clustered water in samples saturated at temperatures between 4° and 100°C, with samples saturated above 23°C, then quenched in water at 23°C (see Fig. 11). Within the limits of detection (10 ppm), no clustered water melting at 0°C was observed in samples saturated at or below 50°C.

5.2 Exploration of water trapped during core extrusion

The polyethylene core is extruded at about 190° to 200°C and is then cooled by traversing a series of water troughs starting at temperatures of 80° to 100°C and descending in temperature to 20°C. When the molten core enters the first trough, water vapor diffuses into the polyethylene to produce a concentration of 100 to 200 ppm near the surface, reducing to about 10 ppm at a depth of 0.2 in. As the temperature of the polyethylene drops below approximately 105°C, crystallization starts and it is hypothesized that noncompatible materials (polar groups, antioxidant, and water) are swept ahead of the crystallizing surfaces. When the temperature decreases further, the clustering of these impurities triggers the precipitation of globules of water near the outer surface of the core. The globules contain traces of water-soluble salts and antiox-
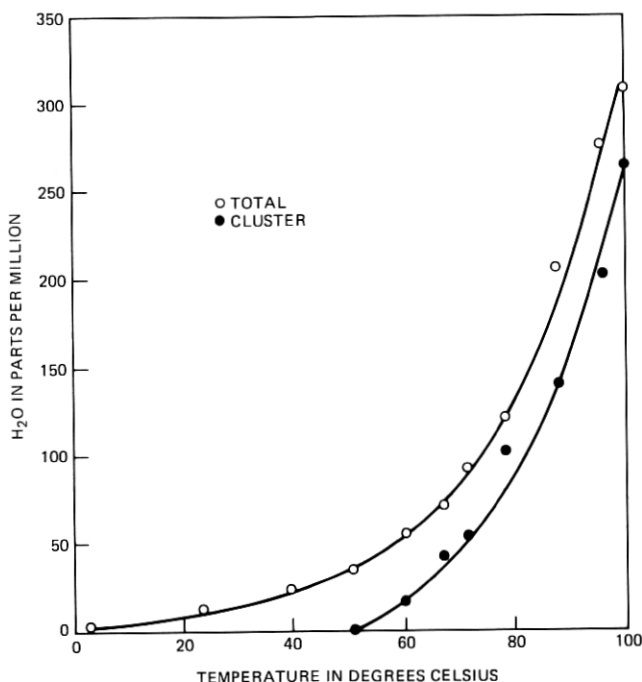
Fig. 11—Saturation content in SG cable.

idant and attract to the polyethylene-water interface any polar groups in the vicinity. Thus, the water droplet conditions its surroundings and produces some small water-filled voids with hydrophilic surfaces. The diffusion coefficient drops sharply with temperature, and very little of the precipitated water can escape from the cable before it reaches room temperature. When the core is exposed to the atmosphere prior to sheathing, the trapped water slowly dries out and if it is left for longer than one week in the air, it will usually recover to a low water content. However, many of the voids will be left with hydrophilic surfaces so that, if exposed to water on the sea bed, they can refill, causing changes in the dielectric loss.

The standard procedure of shaving 0.070 in. (1.78 mm) from the outside of the core removes the more heavily contaminated material but is insufficiently deep to remove all the damaged polyethylene.

5.3 Effects of water on dielectric loss

To determine the effects of water on the dielectric loss of the polyethylene core, numerous experiments have been carried out both on cable and on plaques simulating cable core. It was found that, although water in the vapor phase has a small effect on the dielectric loss below the microwave range, microdroplets as small as 0.1 μm in diameter can have

considerable influence on the loss in the megahertz region. They act as small regions of high permittivity and finite resistivity dispersed in a low-loss dielectric medium. The dielectric response of such a system is governed by relaxation equations and in the simplest case will exhibit a single Debye-type peak whose frequency is mainly dependent on the permittivity and resistivity of the small regions. In the case of the microdroplets, the resistivity of the water will be modified by the presence of soluble impurities such that the peak occurs in the megahertz range. The general behavior is known as the Maxwell-Wagner effect. In practice, there may also be a small increase in loss in the megahertz region due to water in the vapor phase causing an enhancement of the gamma process,[2] which is centered around 1 GHz in polyethylene.

Typical behavior is illustrated in the results of the following experiment, shown in Fig. 12. To simulate the conditions in the outer layer of the core immediately after extrusion and cooling, a series of plaques (2 mm thick) was molded at 180°C. The molten plaques, attached to metal backing sheets, were then dropped into baths of water at 95° to 70°C for 30 minutes. The dielectric loss was measured at frequencies up to 30 MHz as a function of drying time at 23°C and 35-percent relative humidity. The effect of the water on the polyethylene was found by normalizing the times and plotting the excess loss over that for a normal molded plaque cooled in air. A typical example simulating a first cooling trough at 95°C is given in Fig. 12; the initial effect is large, with a peak
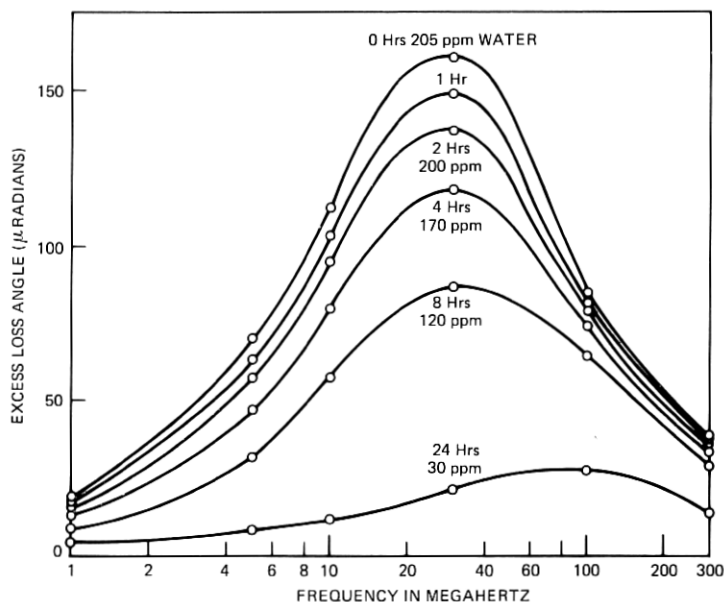

Fig. 12—Increase in loss angle caused by immersing molten plaques in water at 95°C for 30 minutes, plotted as a function of drying time.

excess loss of approximately 160 μrad at 3 MHz for a water content of 245 ppm. The effect decays quite fast so that, after eight hours, the peak excess loss is down to approximately 85 μrad; after twenty-four hours, the peak has shifted up to 8 MHz and is approximately 25 μrad high for a water content of 30 ppm. The experiments on plaques highlight the effect of clustered water on polyethylene, but luckily the influence on the overall attenuation of finished cable is heavily diluted by a number of factors.

The behavior of plaques represents only the outer layers of the core. The inner layers are free from clusters and contain water to the normal saturation level of about 10 ppm. This level remains substantially constant while the outer layer dries down. So whereas the effect of water on the dielectric loss of the outer layer of freshly extruded core is initially very large, the rest of the core is scarcely affected, and the dielectric loss integrated over the whole cross section shows only a small increase. As a rough rule of thumb, the overall change in dielectric loss integrated over the entire SG cable core is about $\frac{1}{10}$ the excess loss of a plaque simulating its outer layer. Taking as an example the results of the plaque experiment given in Fig. 12, the plaque initially exhibited an excess loss of 37 microradians at 30 MHz, decreasing to 12 microradians after 24 hours. The dielectric loss of an equivalent SG core would be increased initially by 3.7 microradians; this would then drop to 1.2 microradians.

In terms of overall cable attenuation, the effect is further diluted by the fact that, at low frequencies, the dielectric loss contributes only a very small proportion of the total loss; even at 30 MHz it contributes only 6 percent. Even so, a 1-μrad change at 30 MHz is equivalent to 26-dB change in an overall system of 3400 miles which, if it occurred on the sea bed, would require that the system be re-equalized at several points along its length.

VI. CABLE AGING

The effects of water introduced during the extrusion process and the changes in loss observed on cable lengths monitored in the factory raised questions about the long-term loss stability of the cable in service. Prior to laying the cable, there were only conjectures of the likely behavior on the sea bed but, in spite of inadequate evidence, it was essential to make some estimate of the possible changes in loss over the 20-year life of the system so that an adequate equalization strategy could be formulated. The only piece of evidence available from measurements on sample cable was that a piece of SG sea-trials cable, laid at 1500 fathoms for 2 years, had aged by 1 μrad at 30 MHz. Using this information and results based on other work, it was predicted that the dielectric loss of the SG cable system would age by −1 to +3 μrad in 20 years. (That is, the uncertainty embraced possibilities ranging from a 1-μrad *decrease* to a 3-μrad *increase* in 20 years.)

As predicted, the TAT-6 system is slowly aging on the sea bed: 346 days after commissioning, the phase delay had increased by about 3.5 μs and 583 days after commissioning the attenuation of the deep-water sections had increased by 21.6 dB at 27.5 MHz. The change of attenuation with frequency is approximately linear. The Requirements and Performance paper in this issue of the B.S.T.J. discusses the time behavior of the observed aging and the use of shore-controlled equalizers to compensate for it.

It is hypothesized that water is entering the TAT-6 cable on the sea bed at the repeater terminations and is traveling along the cable causing compression of the core and expansion of the sheath. The resulting sea-water film between the core and outer conductor acts as a lossy dielectric in series with the polyethylene. This, together with the dimensional changes of the cable structure, will cause an increase in attenuation and a change in phase delay.

It is further hypothesized that, in addition to aging from this cause, water in contact with the core will gradually diffuse into the polyethylene and refill some of the dried microvoids. The rate of diffusion will be very slow at deep-sea pressure and temperature. To confirm that polyethylene with dried cluster sites will reabsorb water, laboratory experiments were carried out on a series of plaques similar to those described in Section 5.3. The plaques were allowed to dry under laboratory conditions for a week (simulating the average time between extruding and sheathing the core), by which time their water contents were less than 10 ppm. They were then exposed to approximately 98-percent humidity, and the resulting changes in loss angle as a function of exposure time were plotted for frequencies up to 30 MHz. The results for a plaque initially conditioned in 95°C water are given in Fig. 13. After exposure for 28 days, the plaque had about 60 ppm of water in it. The experiments are still continuing.

The results have been expressed in Fig. 14 in terms of overall attenuation for a complete cable length of 3400 nmi. The curves illustrate how aging from this cause initially might appear linear with frequency and subsequently change shape. In the case of the cable on the sea bed, the effect of exposure to water will proceed at a considerably slower rate than that observed in the experiments. The rate will be limited by the construction of the cable, the longer diffusion paths, and the effects of increased pressure and reduced temperature. Attempts have been made to account for these effects; using data from experiments on short cable samples, they predict similar shapes but about $\frac{1}{3}$ the magnitude of the aging shown. Reabsorption of water into cluster sites will not change the phase delay significantly.

While neither of the two aging mechanisms described above can individually account for all aspects of the observed cable changes, com-
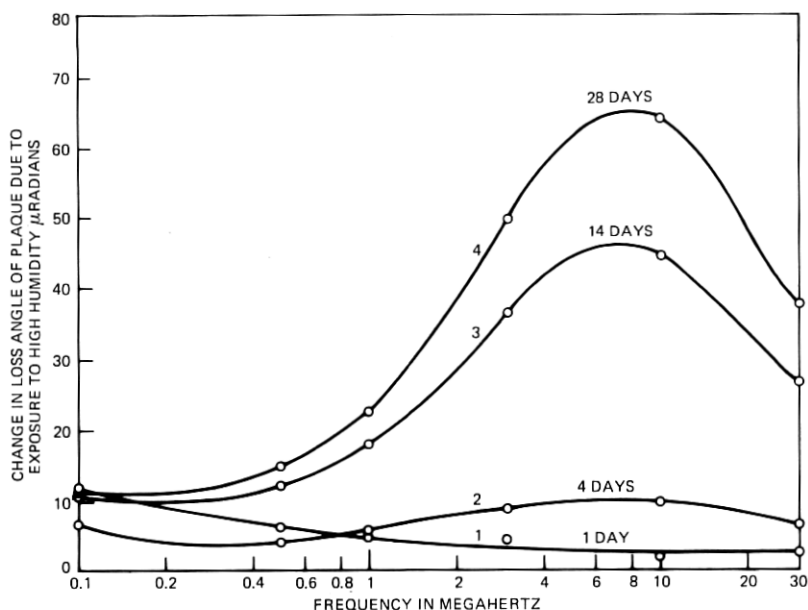
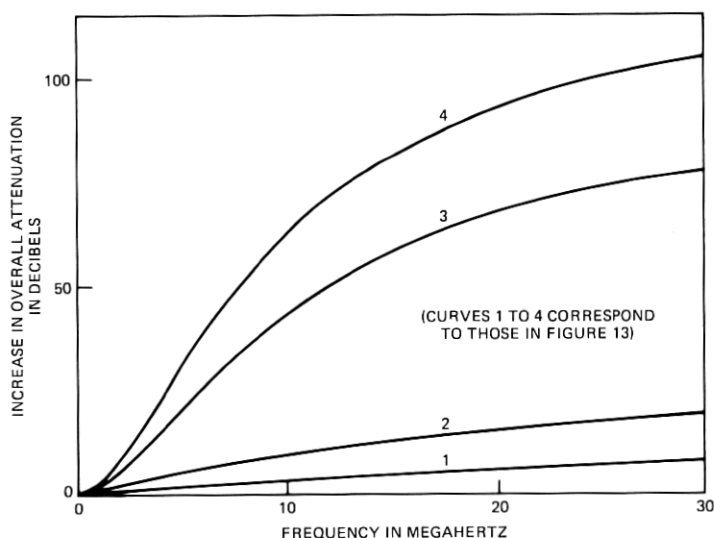Fig. 13—Change in loss angle of plaque on exposure to high humidity after drying for one week.

Fig. 14—Calculated attenuation changes in a 3400-nmi 1.7-in. SG cable assuming dielectric changes due to water.

binations of the two mechanisms can be made to fit the data, including the rate of loss change with time. However, the long-term aging prediction cannot be confirmed without better knowledge of (*i*) the relative movements of core and outer conductor on the sea bed and (*ii*) the effects

of reabsorption of water on the dielectric loss under deep-sea conditions.

VII. LAYING EFFECT

Laying effect is the difference between predicted and actual sea bed transmission losses at the time of lay. Predictions are based on cable and repeater factory measurements that are corrected for estimated sea-bed conditions. A non-zero laying effect can result from errors in factory or shipboard measurements, from cable aging during the period between these measurements; from errors in cable temperature, pressure, and handling coefficients, and from differences between predicted and actual sea-bed conditions at the time of lay. It can also be caused by imperfect knowledge of repeater and equalizer termination losses and impedance discontinuities at the cable-pigtail and the repeater-pigtail interfaces.

In TAT-6, the observed laying effect was remarkably consistent among the several cable lays. It was possible to differentiate between shallow and deep water lays and between cable from different manufacturers. A typical result is shown in Fig. 15 for the first deep water lay. Laying effect was essentially zero at 30 MHz but reached + 0.45 percent at the bottom of the low band. This may be interpreted as a constant cable shape component of + 0.45 percent, which is offset at 30 MHz by a dielectric loss angle at sea bottom which is 4 μrad higher than predicted.*

The average cable shape and linear-loss components of the deep-water laying effect were, from Table III, +0.42 percent and + 4.4 μrad, respectively. Because these errors cancelled at 30 MHz, the resulting misalignment remained well within the equalization range of the OBE but their magnitude is sufficient to warrant an explanation. The difference between the design and the mean sea trials cable pressure coefficient, shown in Fig. 7, suggests a starting point. At 1 MHz, this is +0.16
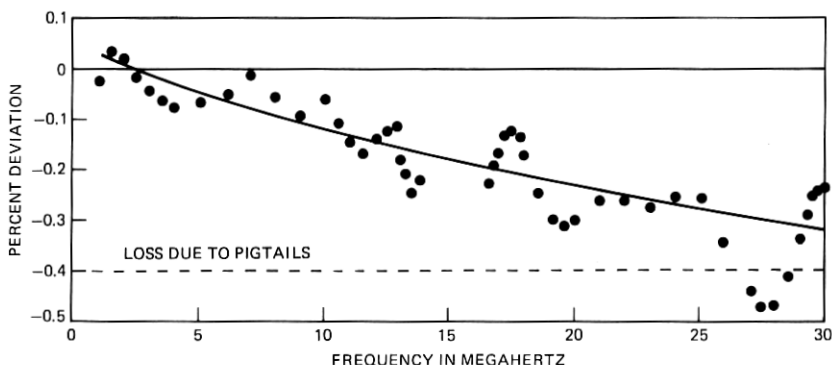

Fig. 15—Lay 1 (deep water) laying effect including 0.4 percent pigtail loss.

* Positive laying effect corresponds to gain relative to prediction.

Table III — TAT-6 cable laying effect

Lay	Cable Length and Supplier (nmi)	Mean Annual Sea-Bed Temperature (°C)	Mean Sea-Bed Depth (kF)	Cable Shape Laying Effect (%)	Linear Loss Laying Effect at 30 MHz (μrad)
Green Hill burial	111 STC/SWC*	10.4†	0.045	+0.30	+1.5
Lay 1	605 STC	2.6	2.19	+0.45	+4.0
Lay 2	634 CDL	2.3	2.67	+0.34	+4.0
Lay 3	640 STC	2.3	2.39	+0.47	+5.5
Lay 4	640 STC	2.9	1.83	+0.51	+4.5
Lay 5	640 STC/CDL	2.6	2.45	+0.31	+4.0
St. Hilaire burial	114 STC	12.8	0.068	+0.44	+2.0

* Cable manufactured by STC and armored by Simplex Wire and Cable Co.
† Actual temperature during the Green Hill burial operation is thought to have been about 2°C higher than annual mean.

percent per kilofathom, enough to explain +0.37 percent of the cable-shape laying effect in deep water. The difference in slope is equivalent to 1.3 μrad per kilofathom at 30 MHz, enough again to account for 3 μrad of the deep water linear-loss laying effect. This leaves only 0.05 percent cable shape and 1.4 μrad of excess loss angle to account for. Together, they correspond to a misalignment of less than ±0.1 percent across the band.

Any further attempts to explain the remaining laying effect are probably not justified by the accuracy of measurement that was possible. However, the loss-angle component could be accounted for by in-factory aging. At least half the cable used in TAT-6 was extruded and cooled under conditions which could cause an increase in loss angle of 2 μrad after 6 months' storage (see Fig. 9). The remaining cable shape effect could also be accounted for quite easily by an error in the air-gap coefficient. Analysis of factory transmission measurements, including study of any change due to cable turnovers, suggests that the average air-gap at 10°C was less than the figure of 0.002-in. (0.051 mm) adopted for the final design. Assuming there is no air gap present when the cable is on the sea bed, then the change in air gap from ship to sea bed will be less than expected and could reduce the cable-shape laying effect by as much as 0.2 percent.

VIII. CABLE TERMINATIONS

Terminations, frequently called couplings, are used on each end of each cable section to interface the cable to the repeater or equalizer. They must perform the following functions:

(*i*) Transfer tensile loads from the strength member of the cable to the repeater or equalizer end cone.

(*ii*) Provide a signal path between the cable and the coaxial pigtail wire which connects the termination to the repeater or equalizer.

(*iii*) Provide sufficient flexibility to permit handling over 9-ft diameter drums and sheaves on cable ships.

(*iv*) While performing the functions above, be capable of withstanding full sea-bottom pressure and the full system dc operating voltage.

Terminations used on armorless cable differ somewhat in requirements and configuration from those used on armored cable, so it is useful to discuss them separately.

8.1 Terminations for armorless cable

The 8G coupling is used on armorless cable. The specific performance requirements to achieve the functions listed above are:

(*i*) 40,000-lb_f (177.9 kN) tensile capability.

(*ii*) 600 in.-lb_f (67.8 m-N) torque capability at maximum tensile load.

(*iii*) At least 35-dB structural return loss from each end.

(*iv*) Capability to allow at least a 45-degree angle between the cable and the repeater or equalizer axis.

(*v*) 7000-V dc capability at both possible polarities with no breakdown and no noise generation in the transmission band.

(*vi*) Capability to withstand 12,000 pounds per square inch (816 atmospheres) sea pressure.

Figure 16 illustrates the design of the 8G coupling. The center strand strength member of the cable is terminated in epoxy in the termination cone. This in turn is glued to a ceramic ring, and the entire assembly is encapsulated in polyethylene. This molded unit is then placed inside the cone housing which attaches to the gimbal mechanism. The gimbal in turn attaches to the gimbal housing and clamp ring, which threads onto the end cone of the repeater or equalizer. In this way, a tensile load in the cable strand is transferred to the repeater or equalizer housing.

Two half-slots are formed in the polyethylene which encapsulates the strand termination. Two keys, part of the cone housing cap, engage these slots to prevent rotation of the anchor mold assembly and provide the required torque capability.

The molded polyethylene layer between the ceramic of the termination assembly and the cone housing is dimensioned to be thin enough to
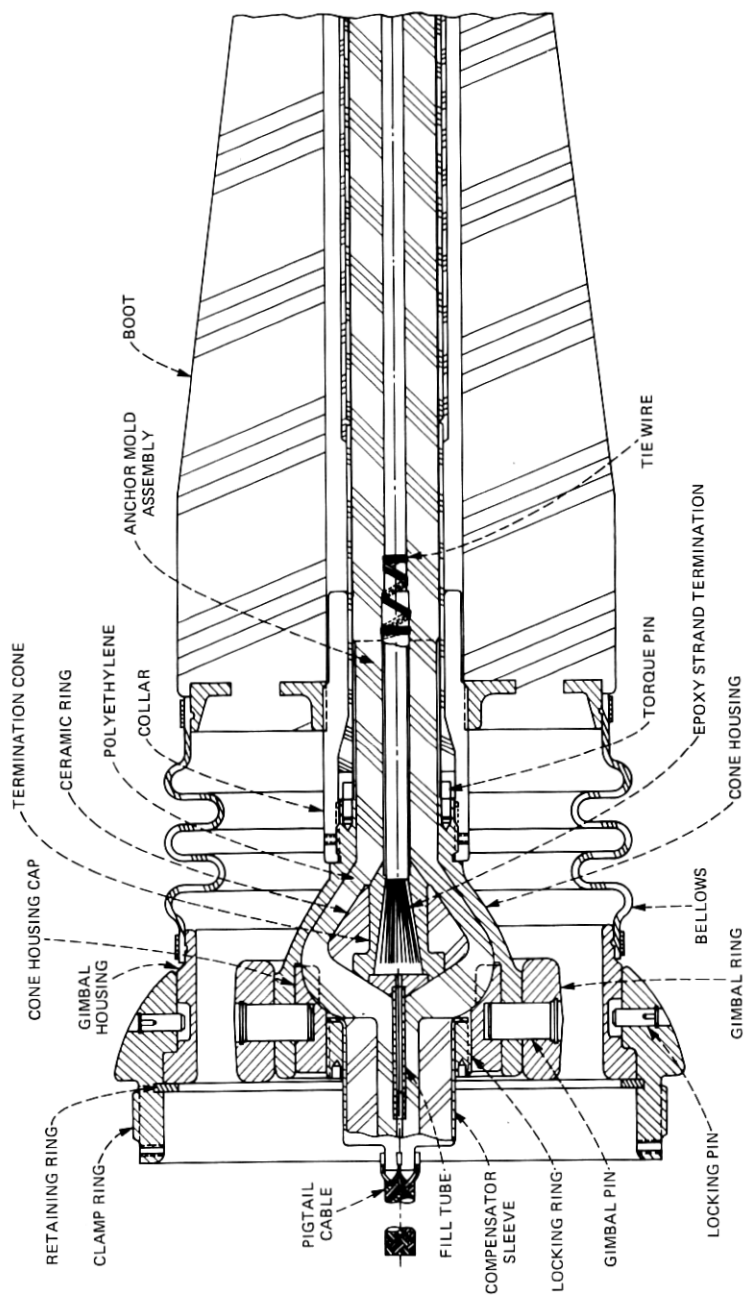
Fig. 16—SG armorless cable coupling.

Labels (clockwise from top):

BOOT

ANCHOR MOLD ASSEMBLY

TIE WIRE

EPOXY STRAND TERMINATION

TORQUE PIN

CONE HOUSING

BELLOWS

GIMBAL RING

LOCKING PIN

GIMBAL PIN

LOCKING RING

COMPENSATOR SLEEVE

FILL TUBE

PIGTAIL CABLE

CLAMP RING

RETAINING RING

CONE HOUSING CAP

GIMBAL HOUSING

TERMINATION CONE

CERAMIC RING

POLYETHYLENE

COLLAR

support the required tensile load and thick enough to provide the high-voltage capability stated above. Within these constraints, it was not possible to achieve the required return loss in the anchor mold assembly as molded. The structure showed excessive capacitance with respect to 50 ohms, so more inductance was needed. To provide this, the large polyethylene sleeve was added at the end of the anchor mold assembly.

The tube on the end of the termination assembly opposite the strand is used for introducing the terminating epoxy into the cone; thus, it must be kept open until the termination is attached to the cable. Since the anchor mold assembly is provided to the cable factory in overmolded condition, the tube must extend outside the molded volume. For this reason, the compensating sleeve could not be made a part of the anchor mold assembly. Instead, it is a separate part which is added after the epoxy termination is complete. The inner conductor of the coaxial pigtail cable is crimped and soldered into the end of the tube and the joint overmolded.

On the opposite end of the anchor mold assembly, the inner conductor of the cable is attached to the conductor tube of the assembly by three turns of three wires to allow for some axial motion under load without loss of continuity. The outer conductor is dimensioned to maintain the 50-ohm cable characteristic impedance up to the termination assembly.

By careful impedance control where possible and by use of the compensating sleeve, the return loss requirement was satisfied.

The gimbal mechanism is so designed that it provides slightly more than 45 degrees of motion between the cable and the repeater or equalizer axis. The bellows is provided to accommodate the gimbal motion while keeping foreign material out of the gimbal mechanism.

The entire termination outside the molded polyethylene is open to sea water, so the sea pressure produces only an additive hydrostatic compression in the various parts. Similarly, the molded assembly is essentially solid so that sea pressure has no detrimental effect.

All the metal parts are made from either copper or copper-beryllium to prevent electrolytic corrosion in sea water.

The large rubber boot serves to limit cable bending radius at the termination and to help guide the whole assembly through the cable machinery on the cable ship.

8.2 Terminations for armored cable

Requirements for the couplings for armored cables differ from those stated above primarily in the tension and torque values. Both the 1-inch (25.4 mm) shielded armored and the 1.7-inch (43.2 mm) single-armored cables have strengths well in excess of 100,000 lb$_f$ (445 kN). After careful

analysis, it was decided that the kind of coupling structure necessary to make the coupling as strong as the cable was unreasonable from both a fabrication and a cost standpoint. Consequently, it was decided to limit the coupling capability to:

(i) 100,000 lb$_f$ (445 kN) tension.

(ii) 25,000 lb$_f \cdot$in. (2825 N$\cdot$m) torque.

In addition, in the couplings for armored cable, the tensile load must be carried from the steel armor wires to the copper-beryllium repeater housing. To prevent corrosion in sea water, special attention must be paid to electrically isolating these two materials from each other at some point while maintaining the tension and torque-carrying capability.

Figure 17 shows the 8N coupling which is used with 1.7-in. (43.2 mm) single-armored cable. The 8P coupling, which is used with 1.0-in. (25.4 mm) shielded-armored cable, is very similar to the 8N, differing only in the details in the round nut assembly that must change with cable diameter.

As in previous cable systems, double-armored cables are terminated as single-armored, the outer armor layer being lashed off outside the coupling.

The strength termination is achieved by crimping a ferrule onto the end of each armor wire. The terminated wires are then placed into the slots of the armor ring against which the ferrules bear. The load is transferred by a yoke arrangement through plastic insulators from the steel armor ring to the copper-beryllium armor housing. The plastic insulators prevent electrolytic corrosion between the dissimilar metals.

To carry the required torque, the armor housing is threaded into a copper-beryllium bushing and secured with a key in the threads. The outside of the bushing is hexagonal in shape and mates, through a plastic insulator, with the hexagonal interior profile of the steel armor ring housing. Similarly, the interface surface between the armor ring housing and the armor ring is hexagonal for torque transfer.

Since most of the strength is in the armor wires, a strength termination is not required for the strand. A direct connection is thus made between the cable inner conductor and the coaxial pigtail inner conductor. The joint is overmolded to provide a transition from the cable to the pigtail outer diameter. The round nut assembly provides a connection between the cable outer conductor and the special outer conductor insert designed to accommodate the diameter transition. This transition joint provides the required return loss.

Other features of the armored coupling such as the gimbal, the bellows, and the rubber boot serve the same functions as described in connection with the armorless cable coupling.

In summary, using the designs described above, the 8G, 8N, and 8P couplings met or exceeded all design requirements.
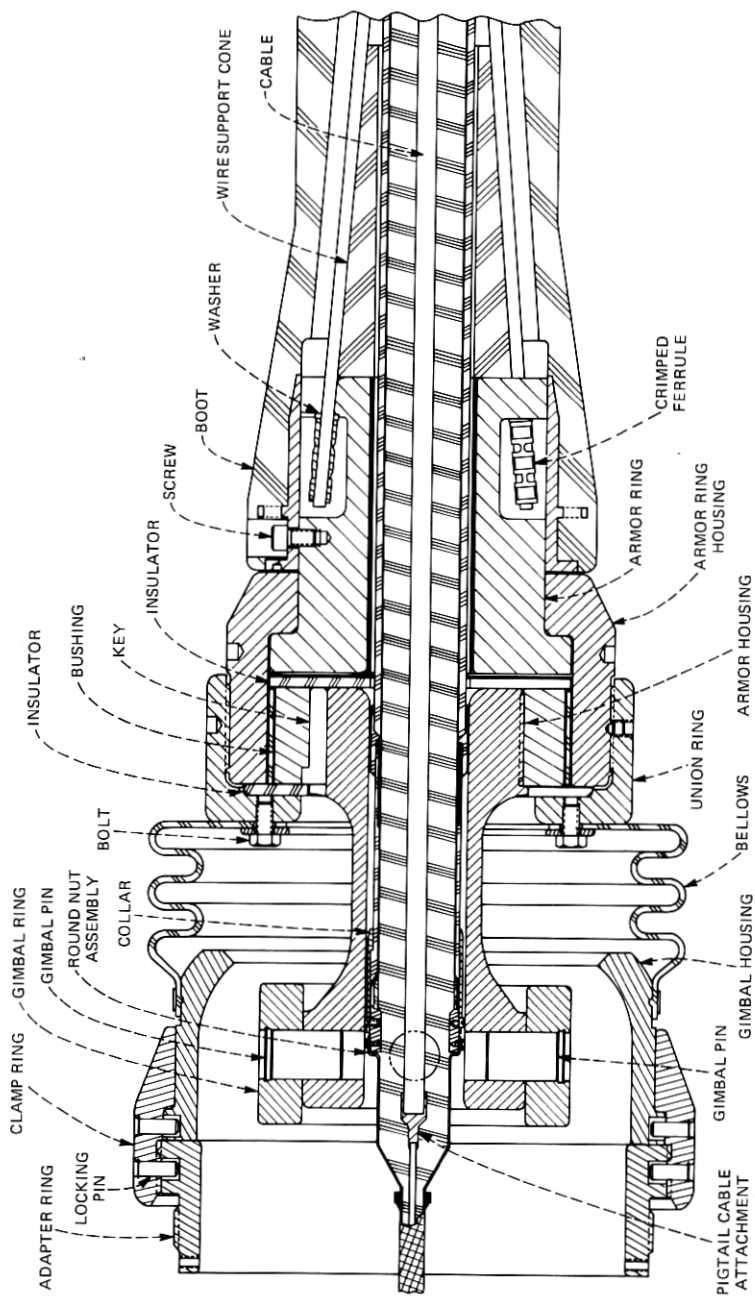
Fig. 17—Typical SG armored cable coupling.

8.3 Pigtail cable

The coaxial pigtail cable mentioned above, which connects the terminated cable to the repeater, has an outer diameter over the insulation of 0.500 in. (12.7 mm) and an inner conductor diameter of 0.146 in. (3.71 mm). These dimensions, used in standard formulas, do not provide a 50-ohm structure. The outer conductor is a copper braid with 0.020-in. (0.51 mm) diameter wires. These wires are much larger than those used in standard braids (typically, 0.007 in. (0.18 mm) diameter), but are required to allow for some loss of material due to corrosion while maintaining continuity. Because these larger wires are used, the outer conductor current is effectively approximately 0.010 in. (0.25 mm) outside the outer surface of the polyethylene insulation. The 0.146-in. (3.71 mm) inner conductor compensates for this effective increase in outer diameter. The braid is covered with heat-shrinkable tubing to hold it in place and to limit water flow for corrosion protection.

When the pigtail is placed in sea water, the conductivity of the water causes a small reduction in the effective coaxial outer diameter, which changes the characteristic impedance of the structure. This change must be accounted for when correlating "wet" and "dry" transmission measurements.

IX. ACKNOWLEDGMENTS

REFERENCES

1. "SF Submarine Cable System," B.S.T.J., *49*, No. 5 (May–June 1970), pp. 601–825.
2. N. G. McCrum, B. E. Read, and G. Williams, *Anelastic and Dielectric Effects in Polymeric Solids*, New York: Wiley, 1967, Chapter 10.